J Electr Eng Technol.2017; 12(5): 1754-1763
http://doi.org/10.5370/JEET.2017.12.5.1754

ISSN(Print) 1975-0102
ISSN(Online) 2093-7423

Fault Location for Incomplete-Journey Double-Circuit Transmission Lines on Same Tower Based on Identification of Fault Branch

Shoupeng Wang†, Dongmei Zhao* and Liqun Shang**

Abstract – This paper analyses the characteristics of incomplete-journey double-circuit transmission lines on the same tower formed by single-circuit lines and double-circuit lines, and then presents a fault location algorithm based on identification of fault branch. With the relationship between the three-phase system and the double-circuit line system, a phase-mode transformation matrix for double-circuit lines can be derived. Based on the derived matrix, the double-circuit lines with faults can be decoupled, and then the fault location for an incomplete-journey double-circuit line is achieved by using modal components in the mode domain. The algorithm is divided into two steps. Firstly, the fault branch is identified by comparing the relationships of voltage amplitudes at the bonding point. Then the fault location, on the basis of the identification result, is calculated by using a two-terminal method, and only the fault distance of the actual fault branch can be obtained. There is no limit on synchronization of each terminal sampling data. The results of ATP-EMTP simulation show that the proposed algorithm can be applied within the entire line and can accurately locate faults in different fault types, fault resistances, and fault distances.

Keywords: Power system, Double-circuit transmission line, Fault location, Phase-mode transformation, Fault branch

1. Introduction

Double-circuit transmission lines on the same tower, characterizing with a narrow corridor, a strong transmission capacity, and remarkable investment benefits, can greatly improve security, reliability, and economy of power grid [1,2]. As double-circuit transmission lines are used widely in engineering, various methods for locating faults on double-circuit lines have been proposed [3-10]. The algorithms based on electrical components can be divided into two categories: one-terminal and two-terminal fault location methods. The one-terminal methods [3-5] use only one terminal data, which is severely affected by fault resistances and system impedances. The two-terminal methods [6-10] can eliminate the influence of fault resistances and system impedances in principle as a result of applying two-terminal data. As for decoupling methods, the majority of the existing fault location algorithms use the six-sequence component method. Especially, the differential component net with zero of bus voltages of two terminals, has attracted widely attention [8]. However, the differential component net does not exist in the case of the symmetrical cross line fault, thus the fault location cannot be achieved.

† Corresponding Author: School of Electrical and Electronic Engineering, North China Electric Power University, Beijing, China. (wsp_ep@yahoo.com)
* School of Electrical and Electronic Engineering, North China Electric Power University, Beijing, China. (zhao-dm@ncepu.edu.cn)
** School of Electrical and Control Engineering, Xi'an University of Science and Technology, Xi'an, China. (shanglq@xust.edu.cn)
Received: January 8, 2017; Accepted: May 11, 2017

At present, the above researches are mainly based on complete-journey double-circuit lines with the common bus, however, a variety of incomplete-journey double-circuit lines on the same tower have been spawned in engineering because of different transmission requirements and geographical environments [11-14]. These incomplete-journey lines partially adopt the same tower structure. For instance, the outlet terminals of the line are set up on the same tower and common bus, the middle part is divided into two independent single-circuit lines, and the end part is connected to two different substations; the front and back parts of the line are divided into two separate single-circuit lines, and the middle part is set up on the same tower, etc. A fault location method for the incomplete-journey line based on a lumped parameter model presented in [13], cannot be used to localize symmetrical faults and neglects the influence of the distributed capacitance. In [14], the proposed algorithm based on a distributed parameter model is described with the consideration of the distributed capacitance. Although it shows high accuracy for various fault conditions, the method has problem with synchronization of sampling data.

Compared with the large number of fault location methods for complete-journey double-circuit lines, the research of incomplete-journey lines is rare. There are various differences between the incomplete-journey and the complete-journey lines not only in fault types but also in line structures. Therefore, this paper describes a fault location method for the incomplete-journey line consisting of a double-circuit line and two single-circuit lines, so as to

provide thoughts for methods based on different structures of incomplete-journey lines.

With the relationship between the three-phase system and the double-circuit line system, a phase-mode transformation matrix for double-circuit lines can be derived. Based on the derived matrix, the double-circuit lines with faults can be decoupled, then the fault location is achieved by using modal components in the mode domain. The algorithm is divided into two steps. Firstly, the fault branch is identified by comparing the relationships of voltage amplitudes at combination. Then according to the result of the judgment, the fault location is completed by using a two-terminal iterative search method, and only the fault distance of the actual fault branch can be obtained. As shown in a large number of simulation results, the proposed algorithm is feasible and effective.

2. Line Model and Decoupling Calculation for Incomplete-Journey Double-Circuit lines

2.1 Line prototype

Compared with complete-journey transmission lines on the same tower, incomplete-journey lines have differences in fault types and in line structures. The incomplete-journey line partially adopts the same tower structure and exists two single-circuit lines. The terminals of two single-circuit lines are connected to different substations respectively, so the lengths of two single-circuit lines are not the same. Therefore, the incomplete-journey line cannot be completely regarded as a double-circuit line or two independent single-circuit lines [14]. On the same tower section, voltages and currents of the differential component net cannot be reacted in the two single-circuit lines, and electrical components of the single-circuit lines with faults are also quite difficult to be reflected in the double-circuit line.

A simplified model of incomplete-journey double-circuit lines is shown in Fig. 1, whose branches are perfectly transposed. Side M of the model is set up with a double-circuit line, whose outlet terminals have the same bus; the middle part is divided into two single-circuit lines which are connected to two different substations respectively.

As shown in Fig. 1, line I and II of side M are set up on the common bus, and terminal T of line I and II are connected to the substations of side N and P respectively. Z_m, Z_n, and Z_p indicate the system equivalent impedances of side M, N and P individually, and $\dot{E}_m$, $\dot{E}_n$, and $\dot{E}_p$ indicate the equivalent sources for side M, N and P separately.

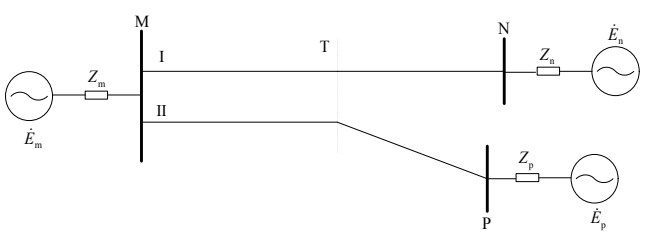

Fig. 1. Schematic of an incomplete-journey double-circuit transmission line

2.2 Decoupling calculation

In the system shown in Fig. 1, the single-circuit line has the interphase coupling, and the double-circuit line has both interphase and line-to-line couplings. Therefore, the decoupling calculation is required before fault analysis, and the fault location can stay immune to fault types via correctly choosing the modal electrical components.

The transmission line is completely under the condition of transposition, its structure and parameters are symmetrical, and the parameter matrix is balanced. For the three-phase system, the relationship between three-phase voltages and currents can be expressed as:

$$\begin{pmatrix} \dot{U}_{\mathrm{mnA}} \\ \dot{U}_{\mathrm{mnB}} \\ \dot{U}_{\mathrm{mnC}} \end{pmatrix} = \begin{pmatrix} Z_S & Z_M & Z_M \\ Z_M & Z_S & Z_M \\ Z_M & Z_M & Z_S \end{pmatrix} \begin{pmatrix} \dot{I}_{\mathrm{mnA}} \\ \dot{I}_{\mathrm{mnB}} \\ \dot{I}_{\mathrm{mnC}} \end{pmatrix} \tag{1}$$

namely, $\dot{\mathbf{U}}_{\mathrm{mnA}} = \mathbf{Z}\dot{\mathbf{I}}_{\mathrm{mnA}}$, the balance parameter matrix is **Z**, i.e.,

$$\mathbf{Z} = \begin{pmatrix} Z_S & Z_M & Z_M \\ Z_M & Z_S & Z_M \\ Z_M & Z_M & Z_S \end{pmatrix},$$

where, Z_S indicates the self-impedance of the line, and Z_M indicates the mutual-impedance. A coupling relationship between phases can be seen from **Z**.

The phase-mode transformation matrices, commonly used for the decoupling calculation, have symmetric component, Karenbauer, Wedpohl, and Clarke transformations, etc [15-16]. The symmetric component can employ positive sequence components to locate various types of short-circuit faults, but its matrix contains complex factors, which increases the amount of calculation. Karenbauer's, Wedpohl's and Clarke's matrices are all the real numbers, which feature with simple computation and less amount of calculation. But at some fault situation, their modal transformations cannot use a single modal component to locate faults according to analysis in [17]. For example, modulus 1 obtained by Clarke's and Wedpohl's matrices cannot locate faults for the non-grounding fault between phase A and C, so do modulus 2 for the grounding fault of phase B; modulus 1 obtained by Karenbauer's matrix cannot locate faults for the grounding fault of phase C, so do modulus 2 for the grounding fault of phase B.

The mathematical essence of decoupling is to seek a phase-mode transformation matrix to make the balance parameter matrix diagonalized. In [17], a single-circuit line

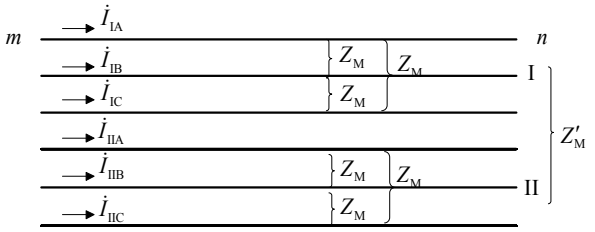

Fig. 2. Schematic of a double-circuit transmission line

can be decoupled by using matrix **T**,

$$\mathbf{T}=\frac{1}{15}\begin{pmatrix}5 & 5 & 5\\ 5 & -1 & -4\\ 5 & -4 & -1\end{pmatrix}.$$

The single-circuit line with mutual inductances can be decoupled by using **T**, and modulus 0, 1, and 2 can then be obtained. Modulus 1 and 2 exist whatever short-circuit fault types occur [17], so modulus 1 or 2 can be used to locate faults, which can overcome the shortcomings of Karenbauer's, Wedpohl's, and Clarke's matrices.

Compared with single-circuit lines, double-circuit lines have not only the interphase coupling, but also the line-to-line coupling.

A model of transposed double-circuit lines is shown in Fig. 2. The interphase impedances of line I or II are the same, namely, Z_M; the impedances between line I and II are also the same, namely, Z'_M; the self-impedance of each line is Z_S. The relationship between voltages and currents is as follows:

$$\begin{pmatrix}\dot{U}_{IA}\\ \dot{U}_{IB}\\ \dot{U}_{IC}\\ \dot{U}_{IIA}\\ \dot{U}_{IIB}\\ \dot{U}_{IIC}\end{pmatrix}=\begin{pmatrix}Z_S & Z_M & Z_M & Z'_M & Z'_M & Z'_M\\ Z_M & Z_S & Z_M & Z'_M & Z'_M & Z'_M\\ Z_M & Z_M & Z_S & Z'_M & Z'_M & Z'_M\\ Z'_M & Z'_M & Z'_M & Z_S & Z_M & Z_M\\ Z'_M & Z'_M & Z'_M & Z_M & Z_S & Z_M\\ Z'_M & Z'_M & Z'_M & Z_M & Z_M & Z_S\end{pmatrix}\begin{pmatrix}\dot{I}_{IA}\\ \dot{I}_{IB}\\ \dot{I}_{IC}\\ \dot{I}_{IIA}\\ \dot{I}_{IIB}\\ \dot{I}_{IIC}\end{pmatrix} \quad (2)$$

When using the phase-mode transformation matrix in [18] to perform decoupling calculation, the first step is to decouple the interphase coupling, leading to only the 0 modulus coupling in the double-circuit line. Then the line-to-line decoupling of the double-circuit line can be achieved via decoupling the 0 modulus coupling. Since the calculation of the line-to-line decoupling is only performed for modulus 0, modulus 1 and 2 of each line are unrelated. When a non-grounding fault occurs on line I or II, the fault location cannot be realized by using electrical components of the non-fault line. For example, when a non-grounding fault occurs on line II, the fault point cannot be found by using modulus 1 of the common component net. Therefore, this paper deals with the above shortcomings successfully by combining the line-to-line decoupling matrix **P** of the six-sequence component method and the above interphase decoupling matrix **T**.

Employing matrix **P** presented in [19], the voltage phasor and the current phasor of the double-circuit line can be decoupled into the common component and the differential component. Eq. (3) can then be obtained as:

$$\dot{\mathbf{U}}_{TF}=\mathbf{P}^{-1}\mathbf{Z}\mathbf{P}\dot{\mathbf{I}}_{TF} \quad (3)$$

where, $\mathbf{P}=\begin{pmatrix}1 & 0 & 0 & 1 & 0 & 0\\ 0 & 1 & 0 & 0 & 1 & 0\\ 0 & 0 & 1 & 0 & 0 & 1\\ 1 & 0 & 0 & -1 & 0 & 0\\ 0 & 1 & 0 & 0 & -1 & 0\\ 0 & 0 & 1 & 0 & 0 & -1\end{pmatrix}$.

Eq. (3) is expanded to obtain Eq. (4),

$$\begin{pmatrix}\dot{U}_{TA}\\ \dot{U}_{TB}\\ \dot{U}_{TC}\\ \dot{U}_{FA}\\ \dot{U}_{FB}\\ \dot{U}_{FC}\end{pmatrix}=\begin{pmatrix}Z_S+Z'_M & Z_M+Z'_M & Z_M+Z'_M & & & \\ Z_M+Z'_M & Z_S+Z'_M & Z_M+Z'_M & & 0 & \\ Z_M+Z'_M & Z_M+Z'_M & Z_S+Z'_M & & & \\ & & & Z_S-Z'_M & Z_M-Z'_M & Z_M-Z'_M\\ & 0 & & Z_M-Z'_M & Z_S-Z'_M & Z_M-Z'_M\\ & & & Z_M-Z'_M & Z_M-Z'_M & Z_S-Z'_M\end{pmatrix}\begin{pmatrix}\dot{I}_{TA}\\ \dot{I}_{TB}\\ \dot{I}_{TC}\\ \dot{I}_{FA}\\ \dot{I}_{FB}\\ \dot{I}_{FC}\end{pmatrix} \quad (4)$$

Transform Eq. (4) into the common and the differential components, that is,

$$\begin{pmatrix}\dot{\mathbf{U}}_T\\ \dot{\mathbf{U}}_F\end{pmatrix}=\begin{pmatrix}\mathbf{Z}_T & \\ & \mathbf{Z}_F\end{pmatrix}\begin{pmatrix}\dot{\mathbf{I}}_T\\ \dot{\mathbf{I}}_F\end{pmatrix} \quad (5)$$

The common and the differential components can be decoupled by using **T** to eliminate the coupling impedances of $\mathbf{Z}_T$ and $\mathbf{Z}_F$, which transforms the common and the differential components into modulus 0, 1, and 2 of the common component net and of the differential component net. The phase-mode transformation matrix $\mathbf{S}=\mathbf{P}\begin{pmatrix}\mathbf{T} & \\ & \mathbf{T}\end{pmatrix}$ can be obtained via combining **P** and **T**, i.e.,

$$\mathbf{S}=\frac{1}{15}\begin{pmatrix}5 & 5 & 5 & 5 & 5 & 5\\ 5 & -1 & -4 & 5 & -1 & -4\\ 5 & -4 & -1 & 5 & -4 & -1\\ 5 & 5 & 5 & -5 & -5 & -5\\ 5 & -1 & -4 & -5 & 1 & 4\\ 5 & -4 & -1 & -5 & 4 & 1\end{pmatrix}.$$

The double-circuit line with mutual inductances can be transformed into six independent modal components with **S**. Matrix **P** makes **S** not only retain the relevance between line I and II, but also have properties like the transformation

matrix of six-sequence component method. For example, when using modulus 1 of the common component net, the fault location can stay immune to fault types. Combined with properties of matrix **T**, modulus 1 and 2 of the common component net decoupled by **S** always exist in various types of short-circuit faults, and can be used to locate various types of faults.

The incomplete-journey double-circuit line in Fig. 1 can be decoupled by using **T** and **S**, and the operation factors of **T** and **S** are all the real numbers. Compared with the complex number operation, the real numbers feature with relatively simple computation and less amount of calculation, which can be applied to both steady and transient analysis.

3. Proposed Fault Location Algorithm

A fault schematic diagram of incomplete-journey double-circuit lines on the same tower is shown in Fig. 3, and each branch is fully transposed. Branch MT is a double-circuit line, including line I and II; branch NT and PT are single-circuit lines; line I and II are respectively connected with NT and PT; MT, NT, and PT are connected together at combination T. Voltages and currents measured from side M, N, and P are $\dot{U}_{\mathrm{M}}$, $\dot{U}_{\mathrm{N}}$, $\dot{U}_{\mathrm{P}}$ and $\dot{I}_{\mathrm{IM}}$, $\dot{I}_{\mathrm{IIM}}$, $\dot{I}_{\mathrm{N}}$, $\dot{I}_{\mathrm{P}}$. $\dot{U}_{\mathrm{T}}$ indicates the voltage of T. $\dot{I}_{\mathrm{IMT}}$, $\dot{I}_{\mathrm{IIMT}}$, $\dot{I}_{\mathrm{NT}}$, and $\dot{I}_{\mathrm{PT}}$ indicate the injection currents of three branches flowing into T individually, and their directions are shown in Fig. 3. The lengths of MT, NT, and PT are l_{m}, l_{n}, and l_{p}. The voltage of point F is $\dot{U}_{\mathrm{F}}$, and the distance from point F to side N is x. A short-circuit fault occurs on point F of NT.

In order to facilitate the following description, this paper names the line consisting of line I of MT and NT as line A, and line II of MT and PT as line B.

The incomplete-journey double-circuit line in Fig. 3 can be decoupled by using matrix **T** and **S** in Section 2.2. Assume that modal voltage components of T calculated from side M, N, and P are $\dot{U}_{\mathrm{T(M)}i}$, $\dot{U}_{\mathrm{T(N)}i}$, and $\dot{U}_{\mathrm{T(P)}i}$. Based on the equation of the uniform transmission line [20], voltages of T in a non-fault state can be expressed as:

$$\dot{U}_{\mathrm{T(M)}i} = \dot{U}_{\mathrm{M}i}\cosh\gamma_{\mathrm{m}i}l_{\mathrm{m}} - Z_{\mathrm{cm}i}\dot{I}_{\mathrm{M}i}\sinh\gamma_{\mathrm{m}i}l_{\mathrm{m}} \tag{6}$$

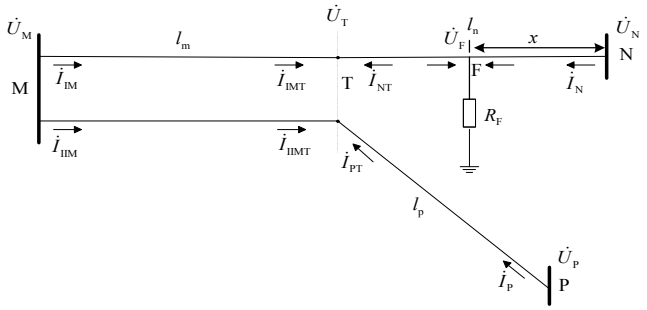

Fig. 3. Fault schematic diagram of an incomplete-journey double-circuit transmission line

$$\dot{U}_{\mathrm{T(N)}j} = \dot{U}_{\mathrm{N}j}\cosh\gamma_{\mathrm{n}j}l_{\mathrm{n}} - Z_{\mathrm{cn}j}\dot{I}_{\mathrm{N}j}\sinh\gamma_{\mathrm{n}j}l_{\mathrm{n}} \tag{7}$$

$$\dot{U}_{\mathrm{T(P)}j} = \dot{U}_{\mathrm{P}j}\cosh\gamma_{\mathrm{p}j}l_{\mathrm{p}} - Z_{\mathrm{cp}j}\dot{I}_{\mathrm{P}j}\sinh\gamma_{\mathrm{p}j}l_{\mathrm{p}} \tag{8}$$

where, i and j indicate modal labels after the double-circuit line and the single-circuit line decoupled separately, i=T0, T1, T2, F0, F1, F2, j = 0, 1, 2; $Z_{\mathrm{cm}i}$ and $\gamma_{\mathrm{m}i}$ indicate the i modulus characteristic impedance and propagation constant of MT; $Z_{\mathrm{cn}j}$, $Z_{\mathrm{cp}j}$ and $\gamma_{\mathrm{n}j}$, $\gamma_{\mathrm{p}j}$ indicate the j modulus characteristic impedances and propagation constants of NT and PT; $\dot{U}_{\mathrm{M}i}$ and $\dot{I}_{\mathrm{M}i}$ indicate the i modulus voltage and current of side M; $\dot{U}_{\mathrm{N}j}$, $\dot{U}_{\mathrm{P}j}$ and $\dot{I}_{\mathrm{N}j}$, $\dot{I}_{\mathrm{P}j}$ indicate the j modulus voltages and currents of side N and P.

Calculate voltages of T from side M, N, and P respectively. The relationships between the phase voltage components and the modal voltage components at T can be expressed as:

$$\begin{pmatrix}\dot{\mathbf{U}}_{\mathrm{TA}}\\ \dot{\mathbf{U}}_{\mathrm{TB}}\end{pmatrix} = \mathbf{S}\begin{pmatrix}\dot{\mathbf{U}}_{\mathrm{T(IM)}}\\ \dot{\mathbf{U}}_{\mathrm{T(IIM)}}\end{pmatrix} = \mathbf{P}\begin{pmatrix}\mathbf{T} & \\ & \mathbf{T}\end{pmatrix}\begin{pmatrix}\dot{\mathbf{U}}_{\mathrm{T(IM)}}\\ \dot{\mathbf{U}}_{\mathrm{T(IIM)}}\end{pmatrix} \tag{9}$$

$$\begin{pmatrix}\dot{\mathbf{U}}_{\mathrm{TA}}\\ \dot{\mathbf{U}}_{\mathrm{TB}}\end{pmatrix} = \begin{pmatrix}\mathbf{T} & \\ & \mathbf{T}\end{pmatrix}\begin{pmatrix}\dot{\mathbf{U}}_{\mathrm{T(N)}}\\ \dot{\mathbf{U}}_{\mathrm{T(P)}}\end{pmatrix} \tag{10}$$

where, $\dot{\mathbf{U}}_{\mathrm{T(IM)}} = (\dot{U}_{\mathrm{T(M)T0}}, \dot{U}_{\mathrm{T(M)T1}}, \dot{U}_{\mathrm{T(M)T2}})^{\mathrm{T}}$ and $\dot{\mathbf{U}}_{\mathrm{T(IIM)}} = (\dot{U}_{\mathrm{T(M)F0}}, \dot{U}_{\mathrm{T(M)F1}}, \dot{U}_{\mathrm{T(M)F2}})^{\mathrm{T}}$ indicate modal voltage components of T calculated from side M; $\dot{\mathbf{U}}_{\mathrm{T(N)}} = (\dot{U}_{\mathrm{T(N)0}}, \dot{U}_{\mathrm{T(N)1}}, \dot{U}_{\mathrm{T(N)2}})^{\mathrm{T}}$ and $\dot{\mathbf{U}}_{\mathrm{T(P)}} = (\dot{U}_{\mathrm{T(P)0}}, \dot{U}_{\mathrm{T(P)1}}, \dot{U}_{\mathrm{T(P)2}})^{\mathrm{T}}$ indicate modal voltage components of T calculated from side N and P; $\dot{\mathbf{U}}_{\mathrm{TA}} = (\dot{U}_{\mathrm{TA}a}, \dot{U}_{\mathrm{TAb}}, \dot{U}_{\mathrm{TAc}})^{\mathrm{T}}$ and $\dot{\mathbf{U}}_{\mathrm{TB}} = (\dot{U}_{\mathrm{TB}a}, \dot{U}_{\mathrm{TBb}}, \dot{U}_{\mathrm{TBc}})^{\mathrm{T}}$ indicate phase voltage components of line A and line B at T.

The modal voltage component amplitudes of T calculated from the three sides are written as $|\dot{\mathbf{U}}_{\mathrm{T(IM)}}|$, $|\dot{\mathbf{U}}_{\mathrm{T(IIM)}}|$, $|\dot{\mathbf{U}}_{\mathrm{T(N)}}|$, and $|\dot{\mathbf{U}}_{\mathrm{T(P)}}|$ respectively. In a non-fault state, there is,

$$\mathbf{P}\begin{pmatrix}\mathbf{T} & \\ & \mathbf{T}\end{pmatrix}\begin{pmatrix}|\dot{\mathbf{U}}_{\mathrm{T(IM)}}|\\ |\dot{\mathbf{U}}_{\mathrm{T(IIM)}}|\end{pmatrix} = \begin{pmatrix}\mathbf{T} & \\ & \mathbf{T}\end{pmatrix}\begin{pmatrix}|\dot{\mathbf{U}}_{\mathrm{T(N)}}|\\ |\dot{\mathbf{U}}_{\mathrm{T(P)}}|\end{pmatrix} \tag{11}$$

Getting rid of **T**, Eq. (11) is simplified as:

$$\mathbf{P}\begin{pmatrix}|\dot{\mathbf{U}}_{\mathrm{T(IM)}}|\\ |\dot{\mathbf{U}}_{\mathrm{T(IIM)}}|\end{pmatrix} = \begin{pmatrix}|\dot{\mathbf{U}}_{\mathrm{T(N)}}|\\ |\dot{\mathbf{U}}_{\mathrm{T(P)}}|\end{pmatrix} \tag{12}$$

Getting rid of **P**, the following relationship can be obtained as:

$$\begin{pmatrix}|\dot{\mathbf{U}}_{\mathrm{T(IM)}} + \dot{\mathbf{U}}_{\mathrm{T(IIM)}}|\\ |\dot{\mathbf{U}}_{\mathrm{T(IM)}} - \dot{\mathbf{U}}_{\mathrm{T(IIM)}}|\end{pmatrix} = \begin{pmatrix}|\dot{\mathbf{U}}_{\mathrm{T(N)}}|\\ |\dot{\mathbf{U}}_{\mathrm{T(P)}}|\end{pmatrix},$$

namely,

$$\begin{pmatrix} |\dot{U}'_{\mathrm{T(M)}0}| \\ |\dot{U}'_{\mathrm{T(M)}1}| \\ |\dot{U}'_{\mathrm{T(M)}2}| \\ |\dot{U}''_{\mathrm{T(M)}0}| \\ |\dot{U}''_{\mathrm{T(M)}1}| \\ |\dot{U}''_{\mathrm{T(M)}2}| \end{pmatrix} = \begin{pmatrix} |\dot{U}_{\mathrm{T(N)}0}| \\ |\dot{U}_{\mathrm{T(N)}1}| \\ |\dot{U}_{\mathrm{T(N)}2}| \\ |\dot{U}_{\mathrm{T(P)}0}| \\ |\dot{U}_{\mathrm{T(P)}1}| \\ |\dot{U}_{\mathrm{T(P)}2}| \end{pmatrix} \tag{13}$$

where, $\dot{U}'_{\mathrm{T(M)}i} = \dot{U}_{\mathrm{T(M)T}i} + \dot{U}_{\mathrm{T(M)F}i}$, i=0,1,2; $\dot{U}''_{\mathrm{T(M)}i} = \dot{U}_{\mathrm{T(M)T}i}$ - $\dot{U}_{\mathrm{T(M)F}i}$, i=0,1,2.

Suppose,

$$\begin{cases} \delta U_{\mathrm{MN}i} = abs\left(\left|\dot{U}'_{\mathrm{T(M)}i}\right| - \left|\dot{U}_{\mathrm{T(N)}i}\right|\right) \\ \delta U_{\mathrm{MP}i} = abs\left(\left|\dot{U}''_{\mathrm{T(M)}i}\right| - \left|\dot{U}_{\mathrm{T(P)}i}\right|\right) \end{cases} \tag{14}$$

When a fault occurs on NT, since there is no fault on line B, voltages of T calculated through Eq. (6) and (8) are exactly the actual modal voltage components, and voltages of T obtained via Eq. (7) are not true. Thus there are $\delta U_{\mathrm{MN}i} > \delta U_{\mathrm{MP}i}$ and $\delta U_{\mathrm{MP}i} \approx 0$. From section 2.2, modulus 1 and 2 of the common component net for the double-circuit line decoupled by **S** always exist, so do modulus 1 and 2 for the single-circuit line. Therefore, the relationships between voltage amplitudes at T can be determined by using modulus 1 and 2 of each line. Then take the average value of the calculated results, in which way the accuracy of identification can be improved. There is,

$$\begin{aligned} &\mathrm{mean}(\delta U_{\mathrm{MN1}}, \delta U_{\mathrm{MN2}}) > \mathrm{mean}(\delta U_{\mathrm{MP1}}, \delta U_{\mathrm{MP2}}) \\ &\frac{\mathrm{mean}(\delta U_{\mathrm{MP1}}, \delta U_{\mathrm{MP2}})}{U_{\mathrm{B}}} \approx 0 \end{aligned} \tag{15}$$

where, mean( ) indicates mean operation function; U_{B} indicates rated voltage.

To facilitate simulation analysis, Eq. (15) is rewritten as:

$$\begin{aligned} &\mathrm{mean}(\delta U_{\mathrm{MN1}}, \delta U_{\mathrm{MN2}}) > \mathrm{mean}(\delta U_{\mathrm{MP1}}, \delta U_{\mathrm{MP2}}) \\ &\frac{\mathrm{mean}(\delta U_{\mathrm{MP1}}, \delta U_{\mathrm{MP2}})}{U_{\mathrm{B}}} < \varepsilon \end{aligned} \tag{16}$$

where, ε is a quite small threshold value and approximately equal to 0.

Similarly, when a fault occurs on PT, there is,

$$\begin{aligned} &\mathrm{mean}(\delta U_{\mathrm{MP1}}, \delta U_{\mathrm{MP2}}) > \mathrm{mean}(\delta U_{\mathrm{MN1}}, \delta U_{\mathrm{MN2}}) \\ &\frac{\mathrm{mean}(\delta U_{\mathrm{MN1}}, \delta U_{\mathrm{MN2}})}{U_{\mathrm{B}}} < \varepsilon \end{aligned} \tag{17}$$

In like manner, when the fault on MT is a single-circuit line fault, if the fault occurs on line I, the relationships between voltage amplitudes at T is Eq. (16); if on line II, it is Eq. (17).

When the fault on MT is a cross-line fault, since there is no fault on NT and PT, voltages of T calculated through Eq. (7) and (8) are true, while through Eq. (6) they are not. Therefore, there are $\delta U_{\mathrm{MN}i} \neq 0$ and $\delta U_{\mathrm{MP}i} \neq 0$. The criterion can be expressed as:

$$\min\left(\frac{\mathrm{mean}(\delta U_{\mathrm{MN1}}, \delta U_{\mathrm{MN2}})}{U_{\mathrm{B}}}, \frac{\mathrm{mean}(\delta U_{\mathrm{MP1}}, \delta U_{\mathrm{MP2}})}{U_{\mathrm{B}}}\right) > \eta \tag{18}$$

where, $\eta \neq 0$, and η is threshold value.

According to the superposition principle, the electrical components of each terminal can be expressed with fault components. Assume that

$$\begin{cases} \Delta U_{\mathrm{MN}i} = abs\left(\left|\Delta\dot{U}'_{\mathrm{T(M)}i}\right| - \left|\Delta\dot{U}_{\mathrm{T(N)}i}\right|\right) \\ \Delta U_{\mathrm{MP}i} = abs\left(\left|\Delta\dot{U}''_{\mathrm{T(M)}i}\right| - \left|\Delta\dot{U}_{\mathrm{T(P)}i}\right|\right) \end{cases},$$

where, i=1,2; $\Delta\dot{U}'_{\mathrm{T(M)}i}$, $\Delta\dot{U}''_{\mathrm{T(M)}i}$, $\Delta\dot{U}_{\mathrm{T(N)}i}$, and $\Delta\dot{U}_{\mathrm{T(P)}i}$ are the fault components of $\dot{U}'_{\mathrm{T(M)}i}$, $\dot{U}''_{\mathrm{T(M)}i}$, $\dot{U}_{\mathrm{T(N)}i}$, and $\dot{U}_{\mathrm{T(P)}i}$. Therefore, the following criterion of identification of fault branch is obtained:

$\mathrm{mean}(\Delta U_{\mathrm{MN1}}, \Delta U_{\mathrm{MN2}}) > \mathrm{mean}(\Delta U_{\mathrm{MP1}}, \Delta U_{\mathrm{MP2}})$

If $\dfrac{\mathrm{mean}(\Delta U_{\mathrm{MP1}}, \Delta U_{\mathrm{MP2}})}{U_{\mathrm{B}}} < \varepsilon$, the fault occurs on line A.

$\mathrm{mean}(\Delta U_{\mathrm{MP1}}, \Delta U_{\mathrm{MP2}}) > \mathrm{mean}(\Delta U_{\mathrm{MN1}}, \Delta U_{\mathrm{MN2}})$

If $\dfrac{\mathrm{mean}(\Delta U_{\mathrm{MN1}}, \Delta U_{\mathrm{MN2}})}{U_{\mathrm{B}}} < \varepsilon$, the fault occurs on line B.

If $\min\left(\dfrac{\mathrm{mean}(\Delta U_{\mathrm{MN1}}, \Delta U_{\mathrm{MN2}})}{U_{\mathrm{B}}}, \dfrac{\mathrm{mean}(\Delta U_{\mathrm{MP1}}, \Delta U_{\mathrm{MP2}})}{U_{\mathrm{B}}}\right) > \eta$, the fault occurs on MT, which is a cross-line fault.

The fault location can be performed with a two-terminal method after determining the fault branch.

When a fault occurs on NT, the modal voltage amplitudes of fault point F calculated from two terminals of NT are equal, there is,

$$\begin{aligned} &\left|\Delta\dot{U}_{\mathrm{N}j}\cosh\gamma_{\mathrm{n}j}x_{\mathrm{n}} - Z_{\mathrm{cn}j}\Delta\dot{I}_{\mathrm{N}j}\sinh\gamma_{\mathrm{n}j}x_{\mathrm{n}}\right| = \\ &\left|\Delta\dot{U}_{\mathrm{IMT}j}\cosh\gamma_{\mathrm{n}j}(l_{\mathrm{n}} - x_{\mathrm{n}}) - Z_{\mathrm{cn}j}\Delta\dot{I}_{\mathrm{IMT}j}\sinh\gamma_{\mathrm{n}j}(l_{\mathrm{n}} - x_{\mathrm{n}})\right| \end{aligned} \tag{19}$$

where, x_{n} is the distance from fault point to side N; $\Delta\dot{U}_{\mathrm{IMT}j}$ and $\Delta\dot{I}_{\mathrm{IMT}j}$, calculated by using fault components of side M, indicate the fault components of modal voltage and current of T on line I; $\Delta\dot{U}_{\mathrm{N}j}$ and $\Delta\dot{I}_{\mathrm{N}j}$ are the fault components of modal voltage and current of side N.

Similarly, when a fault occurs on branch PT or MT, there are Eq. (20) and (21) correspondingly:

$$\left|\Delta\dot{U}_{\mathrm{P}j}\cosh\gamma_{\mathrm{p}j}x_{\mathrm{p}}-Z_{\mathrm{cp}j}\Delta\dot{I}_{\mathrm{P}j}\sinh\gamma_{\mathrm{p}j}x_{\mathrm{p}}\right|= \left|\Delta\dot{U}_{\mathrm{IIMT}j}\cosh\gamma_{\mathrm{p}j}(l_{\mathrm{p}}-x_{\mathrm{p}})-Z_{\mathrm{cp}j}\Delta\dot{I}_{\mathrm{IIMT}j}\sinh\gamma_{\mathrm{p}j}(l_{\mathrm{p}}-x_{\mathrm{p}})\right| \quad (20)$$

$$\left|\Delta\dot{U}_{\mathrm{M}i}\cosh\gamma_{\mathrm{m}i}x_{\mathrm{m}}-Z_{\mathrm{cm}i}\Delta\dot{I}_{\mathrm{M}i}\sinh\gamma_{\mathrm{m}i}x_{\mathrm{m}}\right|= \left|\Delta\dot{U}_{\mathrm{T}i}\cosh\gamma_{\mathrm{m}i}(l_{\mathrm{m}}-x_{\mathrm{m}})-Z_{\mathrm{cm}i}\Delta\dot{I}_{\mathrm{T}i}\sinh\gamma_{\mathrm{m}i}(l_{\mathrm{m}}-x_{\mathrm{m}})\right| \quad (21)$$

where, x_{p} and x_{m} are the distances from fault point to side P and M separately; $\Delta\dot{U}_{\mathrm{IIMT}j}$ and $\Delta\dot{I}_{\mathrm{IIMT}j}$, calculated from side M, indicate the fault components of modal voltage and current of T on line II; $\Delta\dot{U}_{\mathrm{P}j}$ and $\Delta\dot{I}_{\mathrm{P}j}$ are the fault components of side P; $\Delta\dot{U}_{\mathrm{T}i}$ and $\Delta\dot{I}_{\mathrm{T}i}$ indicate the fault components of T calculated from side N and P; $\Delta\dot{U}_{\mathrm{M}i}$ and $\Delta\dot{I}_{\mathrm{M}i}$ are the fault components of side M.

Assume that a fault occurs on line A and the fault branch is NT. As for Eq. (19), since branch MT is not broken, $\Delta\dot{U}_{\mathrm{IMT}j}$ is the actual voltage fault component of T, and $\Delta\dot{I}_{\mathrm{IMT}j}$ is the exact current fault component of line I injected into T. Thus the solution x_{n} of Eq. (19) exists in fault interval (0, l_{n}), namely, x_{n} is the fault distance from fault point to side N.

As for Eq. (21), suppose that $\mathrm{F_m}$ is a fault point of MT and x_{m} is the distance from $\mathrm{F_m}$ to side M. Since voltages and currents of side M are practically measured, the voltage of $\mathrm{F_m}$ calculated through the left of Eq. (21) is actual. When a fault occurs on NT, $\Delta\dot{U}_{\mathrm{T(N)}j}$ and $\Delta\dot{I}_{\mathrm{T(N)}j}$ of T calculated from side N are not true, so $\Delta\dot{U}_{\mathrm{T}i}$ and $\Delta\dot{I}_{\mathrm{T}i}$ are unreal, which leads to the inauthenticity of the calculated voltage of $\mathrm{F_m}$ through the right of Eq. (21). Therefore the solution of Eq.(21) does not exist.

Therefore, when a fault occurs on line A, only Eq. (19) has a solution of x_{n}, which is the fault distance from side N to fault point, and NT is the identified fault branch.

In like manner, when a fault occurs on line B, similar conclusions can be obtained. When the fault on MT is a cross-line fault, the fault distance can be solved via Eq. (21) on the basis of parameters of the double-circuit line. Due to limitations on space, the proof is omitted.

Eq. (19)-(21) are usually solved with the iterative search method [21]. Choosing step Δx and calculating the modal voltage amplitude curves along the whole line, the fault point is the curve intersection. Modulus 1 of the common component net for the double-circuit line and modulus 1 for the single-circuit line exist whatever fault types occur. So Eq. (19)-(21) can be solved using modulus 1 of each line, which can eliminate the impact of fault types.

Note that, when solving Eq. (19) - (21), since the parameters of each branch as shown in Fig. 1 are different, the modal voltages of T need to be performed phase-mode inversion transformation. Namely, the modal voltage and current of the upper branch end, calculated via phase-mode inversion transformation, should be used as the phase voltage and current of the beginning of the next branch.

As for the model in Fig. 1, the fault location method described above needs to be divided into two steps.

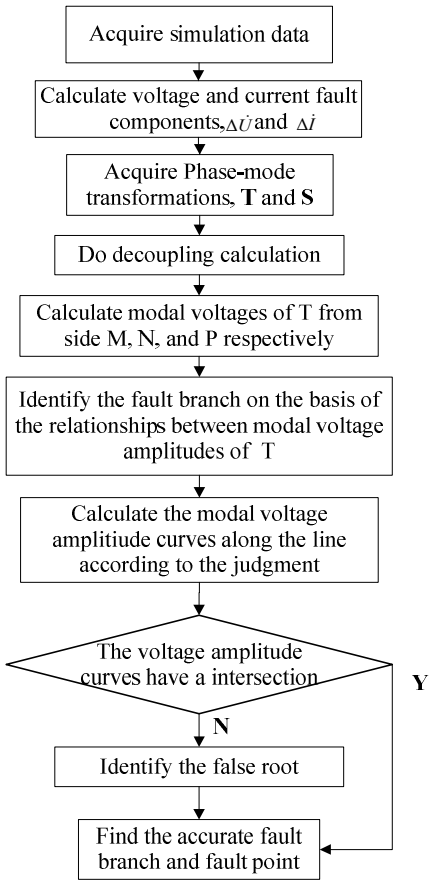

Fig. 4. Procedure of the fault location algorithm

Step 1: Based on parameters of the single-circuit line and of the double-circuit line, the modal voltages of T are calculated. The fault branch can then be identified by comparing the differences between modal voltage amplitudes at T.

Step 2: According to the judgment result, the modal voltage amplitude curves along the line are calculated with the iterative search method. The intersection of curves is namely the fault point, and the branch of locating fault point is the correct identified fault branch.

The solving procedure of the proposed algorithm is shown in Fig. 4.

Therefore, the proposed fault location method employs fault components of modal voltage and current, which can eliminate the influence of the load current. In theory, the sampling data without synchronization only affect the phase of the sinusoidal signal, instead of the amplitude. This paper applies the voltage amplitude distribution to calculate the fault distance, which can eliminate the impact of non-synchronization. In addition, the solving procedure does not involve fault resistances, which makes the fault location stay immune to fault resistances in principle. With the designed selection of electrical components, which exist whatever fault types occur, the proposed algorithm successfully excludes the effect of the specific fault type.

Table 1. Line parameters of the incomplete-journey double-circuit transmission line

Branch	Length (km)	Line impedance(Ω/km)		Line admittance(uS/km)		Mutual coupling	
		Positive sequence	Zero sequence	Positive sequence	Zero sequence	Impedance (Ω/km)	Admittance (uS/km)
MT	250	0.0387+j0.3098	0.1866+j0.7316	j3.7639	j2.0374	0.1476+j0.4217	j0.5398
NT	180	0.0484+j0.3139	0.2067+j0.7193	j3.6143	j1.9222	0	0
PT	120	0.0480+j0.3887	0.1977+j0.8373	j2.9074	j1.7082	0	0

4. Simulation Analysis

To evaluate the performance of the proposed method, faults are simulated on a model of incomplete-journey double-circuit lines on the same tower as shown in Fig. 1. The digital model adopts the distributed parameter model provided by ATP-EMTP, and the parameters are set according to "220kV Overhead Transmission Line Design Technical Regulation" of a Power Grid Corp. The simplified simulation model is shown in Fig. 5.

The fault components of modal voltage and current are used to locate faults, the second cycle after fault is sampled with a sampling frequency of 100kHz, and the filtering technique uses the full-wave Fourier algorithm. The equivalent sources at side M, N, and P are $220\angle 0^\circ$, $220\angle 30^\circ$, and $220\angle 60^\circ$, and the parameters of the model system are shown in Table 1 and 2.

In this paper, ε is a threshold value of the non-fault line when faults of line A or B happen, and its value is approximately equal to 0. η indicates a threshold value when there is a cross-line fault on MT, and its value is larger and not equal to 0. In the following simulation, η and ε are set to 0.1 and 0.03 respectively.

To assess the performance of the proposed phase-mode transformation matrix **S** in section 2.2, locating results in the case of some parts of faults are compared with [18], which are shown in Table 3. The fault point is selected on MT, and the interphase and the grounding fault resistances are all 50Ω. As shown in Table 3, the proposed method can locate various types of short-circuit faults.

Locating results of various fault types are listed in Table 4. The interphase and the grounding fault resistances are all 50Ω, except for the short-circuit fault near combination T which has a high resistance of 300Ω. As for double-circuit lines, the probability of the single-circuit line fault is more than 80%, while the probability of the cross line fault is relatively low. Therefore, only several typical conditions of the cross line fault are presented, such as, I_BII_C, I_BII_{CG}, $I_{AB}II_{BC}$, $I_{AB}II_{BCG}$, I_AII_{BC}, I_AII_{BCG}, I_AII_{ABC} and I_AII_{ABCG}.

Table 4 shows the satisfactory accuracy of the proposed algorithm for different fault types on different branches. What's more, the algorithm stays unaffected by fault types and fault branches. Even if the fault occurs on the vicinity of T, the algorithm can locate faults.

Table 2. System equivalent parameters of the incomplete-journey double-circuit transmission line

Side	System positive sequence impedance(Ω)	System zero sequence impedance(Ω/km)
M	0.0387+j0.3098	0.1866+j0.7316
N	0.0484+j0.3139	0.2067+j0.7193
P	0.048+j0.3887	0.1977+j0.8373

Table 3. Comparison of location results among different methods

Fault type	Fault (km)	Result(km)	
		In [18]	This paper
MI_{ABG}	90	90.1531	89.4522
	160	159.3775	160.3075
MII_{ABC}	90	NaN	90.0436
	160	NaN	160.4799
MI_BII_C	90	90.0778	89.5006
	160	159.3755	159.7031
MII_{BC}	90	NaN	89.6721
	160	NaN	160.1877
$MI_{AB}II_{BCG}$	90	90.5385	89.7356
	160	160.1294	159.8465

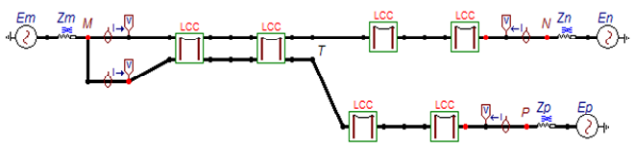

Fig. 5. Simulation model of an incomplete-journey double-circuit line

These locating results of different types of short-circuit faults with different fault resistances are shown in Table 5, and fault points are selected on branch MT. Locating results in Table 5 show that fault resistances have no significant influence on the fault location.

After using non-synchronized data of two-terminal to locate faults, locating results of a single phase-to-earth fault with a fault resistance of 50Ω are shown in Table 6. The fault point is selected on branch NT, and non-synchronized angles are set for $-\pi/3$, $-\pi/60$, 0, $\pi/6$ and $\pi/3$ respectively. Results in Table 6 show that this algorithm can yield the accurate fault distances with different non-synchronized angles.

Table 4. Locating results of different fault types

Fault type	Fault (km)	Fault branch identification	Result (km)	Relative error(%)	Fault type	Fault (km)	Fault branch identification	Result (km)	Relative error(%)
NI_{AG}	70	NT	69.2910	1.0129	MI_{ABG}	90	MT	89.4522	0.6087
	120	NT	119.9908	0.0077		160	MT	160.3075	0.1922
	175	NT	174.9980	0.0011		245	MT	245.6035	0.2463
NI_{AB}	70	NT	69.7965	0.2907	MI_{ABC}	90	MT	89.4484	0.6129
	120	NT	119.8011	0.1657		160	MT	159.3073	0.4329
	175	NT	174.7789	0.1263		245	MT	245.6477	0.2644
NI_{ABG}	70	NT	69.8802	0.1711	$MI_{B}II_{CG}$	90	MT	89.7431	0.2854
	120	NT	119.5806	0.3495		160	MT	159.8386	0.1009
	175	NT	174.8863	0.0650		245	MT	245.7747	0.3162
NI_{ABC}	70	NT	69.8342	0.2369	$MI_{B}II_{C}$	90	MT	89.5006	0.5549
	120	NT	119.7592	0.2007		160	MT	159.7031	0.1856
	175	NT	174.8048	0.1115		245	MT	245.7960	0.3249
PII_{AG}	40	PT	40.0527	0.1318	$MI_{A}II_{BCG}$	90	MT	89.5754	0.4718
	70	PT	69.8438	0.2231		160	MT	160.0666	0.0416
	115	PT	115.6699	0.5825		245	MT	245.1239	0.0506
PII_{AB}	40	PT	39.6975	0.7563	$MI_{A}II_{BC}$	90	MT	89.5759	0.4712
	70	PT	69.7631	0.3384		160	MT	160.1932	0.1207
	115	PT	114.8789	0.1053		245	MT	245.1526	0.0623
PII_{ABG}	40	PT	39.9273	0.1817	$MI_{AB}II_{BCG}$	90	MT	89.7356	0.2938
	70	PT	69.9001	0.1427		160	MT	159.8465	0.0959
	115	PT	114.3632	0.5537		245	MT	245.0091	0.0037
PII_{ABC}	40	PT	39.4530	1.3675	$MI_{AB}II_{BC}$	90	MT	89.3926	0.6749
	70	PT	69.9511	0.0699		160	MT	159.5206	0.2996
	115	PT	114.4160	0.5078		245	MT	245.1116	0.0456
MI_{AG}	90	MT	89.0756	1.0271	$MI_{A}II_{ABCG}$	90	MT	89.6890	0.3456
	160	MT	160.3075	0.1922		160	MT	160.2016	0.1260
	245	MT	244.7871	0.0869		245	MT	245.1148	0.0469
MI_{AB}	90	MT	90.2962	0.3291	$MI_{A}II_{ABC}$	90	MT	89.5864	0.4596
	160	MT	160.1810	0.1131		160	MT	160.2799	0.1749
	245	MT	244.6205	0.1549		245	MT	245.6291	0.2568

Table 5. Location results of different fault resistances

Fault type	Fault (km)	0Ω		50Ω		100Ω		300Ω	
		Result (km)	Relative error(%)	Result (km)	Relative error(%)	Result (km)	Relative error(%)	Result (km)	Relative error(%)
MI_{AG}	90	89.8295	0.1894	89.0756	1.0271	89.3098	0.7669	89.8185	0.2017
	160	159.0272	0.6080	160.3075	0.1922	160.1549	0.0968	160.0195	0.0122
MI_{ABG}	90	90.4420	0.4911	89.4522	0.6087	89.5386	0.5127	89.7514	0.2762
	160	160.3426	0.2141	160.3075	0.1922	160.2310	0.1444	160.7525	0.4703
$MI_{B}II_{CG}$	90	90.6092	0.6769	89.7431	0.2854	89.8448	0.1724	89.8451	0.1721
	160	160.8678	0.5424	159.8386	0.4718	159.8508	0.0933	159.9966	0.0021
$MI_{A}II_{BCG}$	90	90.7143	0.7937	89.5754	0.0416	89.6097	0.4337	89.4366	0.6260
	160	160.5188	0.3242	160.0666	0.2938	159.9781	0.0137	159.9710	0.0181
$MI_{AB}II_{BCG}$	90	90.7354	0.8171	89.7356	0.0959	89.8362	0.1820	89.4795	0.5783
	160	160.8498	0.5311	159.8465	0.3456	159.6563	0.2148	159.8730	0.0794
$MI_{A}II_{ABCG}$	90	90.6252	0.6947	89.6890	0.1260	89.6710	0.3656	89.4035	0.6628
	160	160.8329	0.5206	160.2016	1.0271	160.1418	0.0886	160.1379	0.0862

Table 6. Location results of a single phase-to-earth fault with different non-synchronous angles

Non-synchronous angle	NI_{AG} fault(km)	Result(km)	Relative error(%)
$-\pi/3$	80	79.8004	0.2495
	160	159.6130	0.2419
$-\pi/6$	80	79.3612	0.7985
	160	159.1642	0.5224
0	80	79.8531	0.1836
	160	159.7513	0.1554
$\pi/6$	80	79.5371	0.5786
	160	159.5175	0.3016
$\pi/3$	80	79.6046	0.4942
	160	159.5561	0.2774

5. Conclusion

This paper presents a fault location algorithm for incomplete-journey double-circuit transmission lines on the same tower based on identification of fault branch. The algorithm is divided into two steps. Firstly, the modal voltages of combination T are calculated on the basis of parameters of each branch, and then the fault branch is identified by comparing the differences between modal voltage amplitudes at T. Secondly, according to the prior judgment, the fault location is achieved by using the iterative search method, and only the fault distance of the actual fault branch can be obtained.

The operation factors of the phase-mode transformation matrix in the proposed algorithm are all the real numbers. The real operation features with relatively simple computation and less amount of calculation. Applying fault components of modal voltage and current can eliminate the influence of the load current caused by using the power frequency electrical components. This method is also independent of fault resistances which are not involved in the algorithm principle. There is no need for synchronization of sampling data via calculating voltage amplitudes to find the fault point. The simulation results show that the algorithm can be applied within the entire line, and the accuracy of the fault location is high.

Acknowledgements

This work was supported by the "National Natural Science Foundation of China", no. 51377054, "Natural Science Basic Research Plan of Shanxi Province", no. 2014JM2-5077, and "The Fundamental Research Funds for the Central Universities", no. 2017XS019.

References

[1] H. S. Kim, S. B. Rhee, S. J. Lee, C. H. Kim, Y. S. Kim, "Analysis of Induced Voltage on Telecommunication Line in Parallel Distribution System," *Journal of Electrical Engineering & Technology*, vol. 9, no. 2, pp. 726-732, 2014.

[2] C. Venkatesh, K. S. Swarup, "Steady-state Error Estimation in Distance Relay for Single Phase to Ground Fault in Series-compensated Parallel Transmission Lines," *IET Generation, Transmission & Distribution*, vol. 8, no. 7, pp. 1318-1337, 2014.

[3] W. H. Zhang, U. Rosadi, M. S. Choi, S. J. Lee, I. Lim, "A Robust Fault Location Algorithm for Single Line-to-ground Fault in Double-circuit Transmission Systems," *Journal of Electrical Engineering & Technology*, vol. 6, no. 1, pp. 1-7, 2011.

[4] P. Chaiwan, N. Kang, Y. Liao, "New Accurate Fault Location Algorithm for Parallel Transmission Lines Using Local Measurements," *Electric Power Systems Research*, vol. 108, pp. 68-73, 2014.

[5] G. B. Song, J. L. Suonan, Y. Z. Ge, "An Accurate Fault Location Algorithm for Parallel Transmission Lines Using One-terminal Data," *International Journal of Electrical Power & Energy Systems*, vol. 31, pp. 124-129, 2009.

[6] X. Chen, Y. L. Zhu, X. H. Guo, L. Zhao, Y. F. Gao, "Dual-terminal Asynchronous Fault Location Algorithm for Two Parallel Overhead Lines on Same Pole," *Electric Power Automation Equipment*, vol. 36, no. 5, pp. 87-90, 2016.

[7] S. M. Yeo, W. H. Jang, C. H. Kim, "Algorithm for Fault Location Estimation on Transmission Lines using Second-order Difference of a Positive Sequence Current Phasor," *Journal of Electrical Engineering & Technology*, vol. 8, no. 3, pp. 499-506, 2013.

[8] G. B. Song, J. Suonan, Q. Q. Xu, P. Chen, Y. Z. Ge, "Parallel Transmission Lines Fault Location Algorithm Based on Differential Component Net," *IEEE Transactions on Power Delivery*, vol. 20, no. 4, pp. 2396-2406, 2005.

[9] C. A. Apostolopoulos, G. N. Korres, "Accurate Fault Location Algorithm for Double-circuit Series Compensated Lines Using a Limited Number of Two-end Synchronized Measurements," *International Journal of Electrical Power & Energy Systems*, vol. 42, pp. 495-507, 2012.

[10] N. I. Elkalashy, T. A. Kawady, W. M. Khater, A. M.I. Taalab, "Unsynchronized Fault-Location Technique for Double-Circuit Transmission Systems Independent of Line Parameters," *IEEE Transactions on Power Delivery*, vol. 31, no. 4, pp.1591-1600, 2016.

[11] T. Yu, C. J. Fan, Z. D. Gong, "A Study on Accurate Fault Location Algorithm for Parallel Transmission Line with a Teed Connection," *International Journal of Electrical Power & Energy Systems*, vol. 32, no. 6, pp. 697-703, 2010.

[12] N. Kang, J. X. Chen, Y. Liao, "A Fault-Location Algorithm for Series-Compensated Double-Circuit Transmission Lines Using the Distributed Parameter Line Model," *IEEE Transactions on Power Delivery*, vol. 30, no. 1, pp. 360-367, 2015.

[13] Z. A. Yu, M. Z. Cheng, P. Y. Guo, N. L. Tai, "A New Fault Locating of T-type Transmission Line Consisting of Four Parallel-line and Double Circuit," *Power System Protection and Control*, vol. 42, no. 15, pp. 8-7, 2014.

[14] X. Deng, "Study on Relay Protection and Fault Location New Technology for Parallel Transmission Lines on Same Tower," PhD thesis, *Huazhong University of Science and Technology*, 2012.

[15] A. T. Johns, S. Jamali, "Accurate Fault Location Technique for Power Transmission Lines," *IEE Proceeding C: Generation Transmission and Distribution*, vol. 137, no. 6, pp. 395-402, 1990.

[16] A. T. Johns, S. K. Salman, "Digital Protection for Power Systems," *Peter Peregrinus Ltd.*, London, 1995.
[17] G. B. Song, S. Li, X. N. Kang, D. S. Zhou, Z. L. Yang, J. L. Suonan, "A Novel Phase-mode Transformation Matrix," *Automation of Electric Power Systems*, vol. 34, no. 14, pp. 57-60, 2007.
[18] H. C. Shu, Z. S. Liu, S. X. Peng, "Locating Arc Faults on Coupling Two Parallel Transmission Lines Using the Novel Phase-mode Transformation," *High Voltage Engineering*, vol. 35, no. 3, pp. 480-486, 2009.
[19] Y. Z. Ge, "Principle and Technology of New Protection Relay and Fault Location," *Xi'an Jiaotong University Press*, Xi'an, 2007.
[20] B. Mahamedi, M. Sanaye-Pasand, S. Azizi, J. G. Zhu, "Unsynchronised Fault-Location Technique for Three-terminal Lines," *IET Generation, Transmission & Distribution*, vol. 9, no. 15, pp.2099-2107, 2015.
[21] X. Gui, Z. G. Liu, X. D. Han, Q. Q. Qian, "An Accurate Algorithm of Two-terminal Fault Location Based on the Distribution of Line Voltage along HV Transmission Line," *Proceedings of the CSEE*, vol. 29, no. 19, pp. 63-69, 2009.

Shoupeng Wang He is a Ph.D. candidate in the School of Electrical and Electronic Engineering, North China Electric Power University. He received the B.S. degree in Electrical Engineering and Automation from North China Electric Power University, and his M.S. degree in Electrical Engineering from Xi'an University of Science and Technology. His current interests include analysis, operation and protection of electric power system, and power grid fault diagnosis.

Dongmei Zhao She is a professor and Ph.D. student supervisor of the School of Electrical and Electronic Engineering, North China Electric Power University. She received the B.S. degree in the electric power system and its automation from Wuhan Institute of Hydraulic and Electric Engineering (currently known as Wuhan University), and her M.S. and Ph.D. degree in the electric power system and its automation from North China Electric Power University. Her current interests include analysis, operation and optimization of electric power system, electric power system with new energy sources, applications of artificial intelligence in electric power system.

Liqun Shang He is a professor of the School of electrical and control engineering, Xi'an University of Science and Technology. He graduated from Xi'an JiaoTong University and received his Ph.D. degree in Electrical Engineering. His current interests include analysis and control of electric power system, and electromagnetic transient simulation.